

Article

Highly Stable Zr(IV)-Based Metal-Organic Frameworks with Chiral Phosphoric Acids for Catalytic Asymmetric Tandem Reactions

Wei Gong, Xu Chen, Hong Jiang, Dandan Chu, Yong Cui, and Yan Liu

J. Am. Chem. Soc., **Just Accepted Manuscript** • DOI: 10.1021/jacs.9b02294 • Publication Date (Web): 15 Apr 2019

Downloaded from <http://pubs.acs.org> on April 15, 2019

Just Accepted

"Just Accepted" manuscripts have been peer-reviewed and accepted for publication. They are posted online prior to technical editing, formatting for publication and author proofing. The American Chemical Society provides "Just Accepted" as a service to the research community to expedite the dissemination of scientific material as soon as possible after acceptance. "Just Accepted" manuscripts appear in full in PDF format accompanied by an HTML abstract. "Just Accepted" manuscripts have been fully peer reviewed, but should not be considered the official version of record. They are citable by the Digital Object Identifier (DOI®). "Just Accepted" is an optional service offered to authors. Therefore, the "Just Accepted" Web site may not include all articles that will be published in the journal. After a manuscript is technically edited and formatted, it will be removed from the "Just Accepted" Web site and published as an ASAP article. Note that technical editing may introduce minor changes to the manuscript text and/or graphics which could affect content, and all legal disclaimers and ethical guidelines that apply to the journal pertain. ACS cannot be held responsible for errors or consequences arising from the use of information contained in these "Just Accepted" manuscripts.



ACS Publications

is published by the American Chemical Society, 1155 Sixteenth Street N.W., Washington, DC 20036

Published by American Chemical Society. Copyright © American Chemical Society. However, no copyright claim is made to original U.S. Government works, or works produced by employees of any Commonwealth realm Crown government in the course of their duties.

Highly Stable Zr(IV)-Based Metal-Organic Frameworks with Chiral Phosphoric Acids for Catalytic Asymmetric Tandem Reactions

Wei Gong,[†] Xu Chen,[†] Hong Jiang,[†] Dandan Chu,[†] Yong Cui,^{*,†,‡} and Yan Liu^{*,†}

[†]School of Chemistry and Chemical Engineering and State Key Laboratory of Metal Matrix Composites, Shanghai Jiao Tong University, Shanghai 200240, China

[‡]Collaborative Innovation Center of Chemical Science and Engineering, Tianjin 300072, China

Supporting Information

ABSTRACT: Heterogeneous Brønsted acid catalysts featuring high porosity, crystallinity and stability have been of great interest for both fundamental studies and practical applications, but synthetically they still face a formidable challenge. Here we illustrated a ligand design strategy for directly installing chiral phosphoric acid catalysts into highly stable Zr-MOFs by sterically protecting them from coordinating with metal ions. A pair of chiral porous Zr(IV)-MOFs with the framework formula $[\text{Zr}_6\text{O}_4(\text{OH})_8(\text{H}_2\text{O})_4(\text{L})_2]$ were prepared from enantiopure 4,4',6,6'-tetra(benzoate) and -tetra(2-naphthoate) ligands of 1,1'-spirobiindane-7,7'-phosphoric acid. They share the same topological structure but differ in channel sizes, and both of them demonstrate excellent tolerance towards water, acid and base. Significantly enhanced Brønsted acidity was observed for the phosphoric acids that are uniformly distributed within the frameworks in comparison with the non-immobilized acids. This not only facilitates the catalysis of asymmetric two-component tandem acetalization, Friedel-Crafts and iso-Pictet-Spengler reactions, but also promotes the catalysis of asymmetric three-component tandem deacetalization-acetalization and Friedel-Crafts reactions benefiting from the synergy with exposed Lewis acidic Zr(IV) sites. The enantioselectivities are comparable or favorable compared to those obtained from the corresponding homogeneous systems. The features of high reactivity, selectivity, stability and recyclability for Zr(IV)-MOFs make them hold promise as a new type of heterogeneous acid catalyst for the eco-friendly synthesis of fine chemicals.

INTRODUCTION

To achieve high reactivity and selectivity, great efforts have been devoted to developing heterogeneous Brønsted acid catalysts that are highly porous, crystalline and stable.¹⁻⁵ Conventional solid acids, however, generally lack structural uniformity and possess diverse types of active sites, differing in both activity and selectivity.^{6,7} One class of hybrid solids that can provide exceptional structural uniformity and permanent porosity are metal-organic frameworks (MOFs).⁸ Owing to the highly modular nature and facile tunability, MOFs have shown promising applications in diverse areas.^{9,10} Especially, the discovery of MOFs constructed from high-valent metals such as Zr(IV) and Cr(III) has dramatically increased MOF stability and robustness,¹¹⁻¹⁵ which make them an ideal platform for designing single-site heterogeneous catalysts for important chemical reactions such as asymmetric transformations.¹⁶⁻²⁹ With few exceptions,¹⁶⁻¹⁸ however, the reported chiral MOFs (CMOFs) typically showed limited stability under acidic and alkaline conditions.¹⁹⁻²⁹ Moreover, the dominated majority of them are Lewis acid-type catalysts derived from privileged chiral ligands¹⁶⁻²⁵ and only few are Brønsted acid species that displayed only low to moderate enantioselectivities (6-84% ee).²⁶⁻²⁹ It is difficult to prepare CMOFs with strong Brønsted acid sites (BASs) from sulfonated or phosphonated organo- catalysts because they tend to bind to metal ions and hence lose Brønsted acidity in MOF synthesis.^{30,31} Therefore, the synthesis of highly stable CMOFs with strong BASs remains a big challenge to be addressed. In this work, we demonstrated that catalytically active chiral phosphoric acids can be directly incorporated into robust and porous Zr(IV)-MOFs by sterically protecting them from coordinating with metal ions.

As a class of fairly strong Brønsted acids, chiral phosphoric acids derived from axially chiral biaryls, especially BINOL (1,1'-binaphthol)³² and SPINOL (1,1'-spirobiindane-7,7'-diol)³³ have been proved to be privileged catalysts enabling a broad range of enantioselective reactions involving imines [e.g. Mannich,³⁴ Friedel-Crafts (F-C),³⁵ aza-Diels-Alder³⁶ and Pictet-Spengler (P-S) reactions³⁷]. Compared with the BINOL backbone, the spirocyclic SPINOL possess a geometrically different and more rigid and narrow cavity and enable readily control of the steric and electronic properties of the asymmetric environment of the phosphoric acid catalyst.³⁸ We envisaged that introduction of steric bulky binding functional groups at the 6,6'-positions of the SPINOL backbone may protect phosphoric acids from coordinating to large metal clusters such as $[\text{Zr}_6\text{O}_4(\text{OH})_8(\text{H}_2\text{O})_4]$, whereas the primary functional groups can be linked by metal-connecting units to produce extended networks. Here we reported the construction of two robust Zr(IV)-CMOFs with a topological isostructure from the newly designed enantiopure 4,4',6,6'-tetra(benzoate) and -tetra(2-naphthoate) ligands of 1,1'-spirobiindane-7,7'-phosphoric acid. The uncoordinated phosphoric acids within the frameworks can catalyze asymmetric two-component tandem acetalization, F-C and iso-P-S reactions and can also work with the exposed Lewis acidic Zr(IV) sites to promote asymmetric three-component tandem deacetalization-acetalization and F-C reactions, with enantioselectivity comparable to or surpassing the homogeneous analogs. It should be noted that MOFs have been used in tandem reactions where multiple continuous reactions are combined into one process, but none of them are capable of promoting enantioselective tandem reactions.^{39,40}

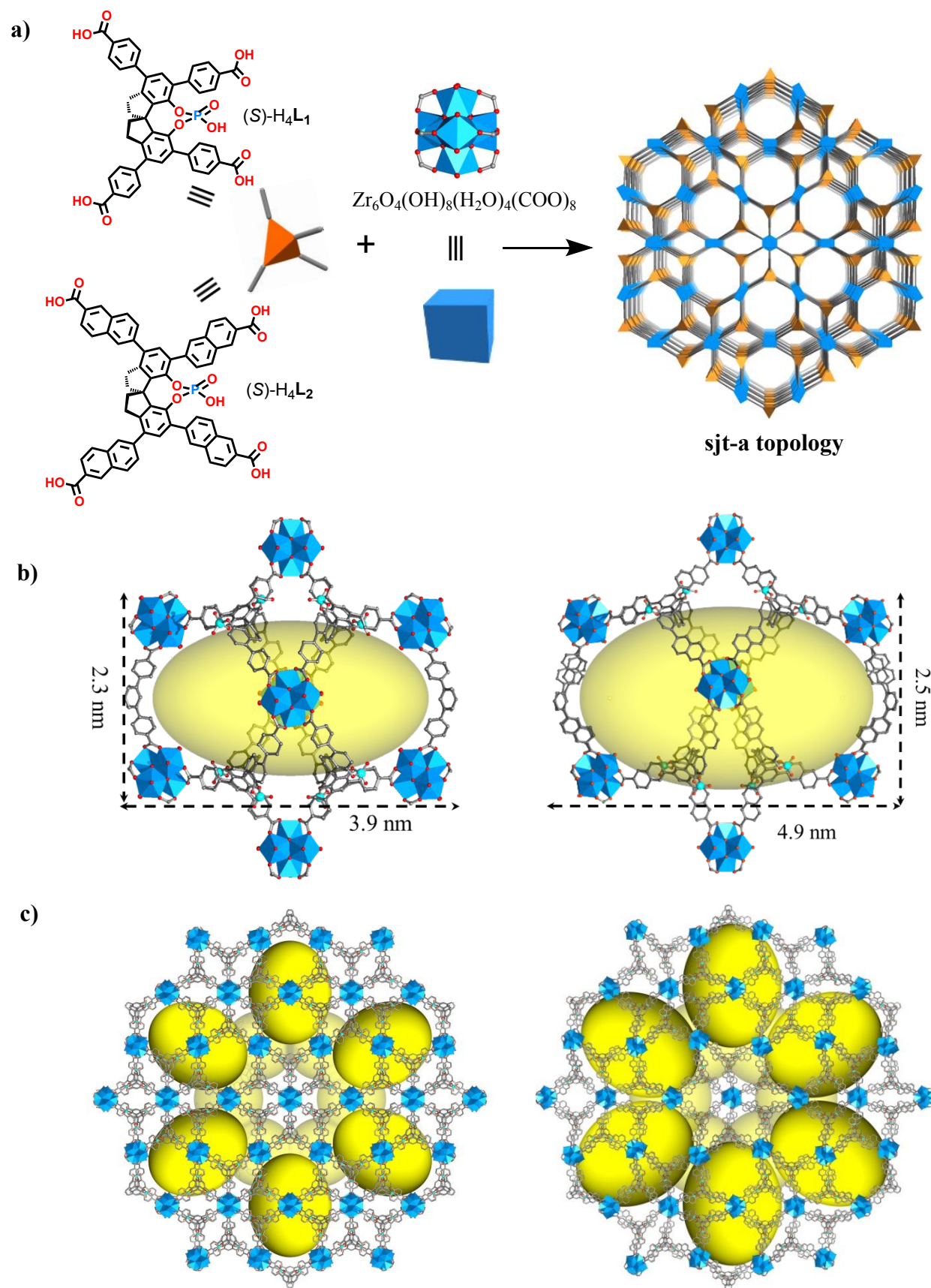


Figure 1. (a) Construction of **Spiro-1** and **Spiro-2** from the Zr_6 clusters linked by H_4L to give the **sjt-a** topology. (b) The hexagonal bipyramid cages and (c) the 3D porous structures in **Spiro-1** (left) and **Spiro-2** (right) viewed along the c-axis. The cavities are highlighted by yellow ellipsoids, and H atoms are omitted for clarity.

RESULTS AND DISCUSSION

Synthesis and Characterization. Most of the reported Zr(IV)-MOFs with tetratopic carboxylate ligands are based on rigid platforms such as porphyrin,¹⁵ tetraphenylethylene,⁴¹ pyrene⁴² and biphenyl.⁴³ All these Zr-MOFs were found to display excellent chemical stabilities and large surface areas. However, tetratopic linkers with inherent chirality have not yet been explored for construction of Zr-MOFs, although synthesis of highly stable MOFs with rich chirality-related functions has been of great concern. The newly designed linker H_4L_1 and H_4L_2 were prepared from enantiopure (*S*)- or (*R*)-SPINOL in four steps in 58% and 47% overall yields, respectively. Heating $ZrCl_4$ and H_4L_1 or H_4L_2 in the presence of formic acid as competing reagent in DMF afforded colorless hexagonal pyramid-shaped crystals of $[Zr_6O_4(OH)_8(H_2O)_4(L_1)_2]$ (**Spiro-1**) or $[Zr_6O_4(OH)_8(H_2O)_4(L_2)_2]$ (**Spiro-2**). They have been fully characterized by a variety of techniques including IR spectroscopy, microanalysis and thermogravimetric analysis (TGA). The phase purity of them was established by comparison of their observed and simulated powder X-ray diffraction (PXRD) patterns.

Single-crystal X-ray diffraction reveals that **Spiro-1** and **Spiro-2** crystallize in different space groups but with the same structural topology. **Spiro-1** crystallizes in the hexagonal chiral space group of $P6_222$ with three-fourths of the formula in the asymmetric unit. There are two different types of eight-connected Zr_6O_8 clusters with D_{4h} or D_{2d} symmetry in the framework (Figure S1). Six Zr atoms are connected by four μ_3 -O and four μ_3 -OH groups to generate $Zr_6(\mu_3-O)_4(\mu_3-OH)_4$ cluster, with four -OH and four H_2O attached as terminal groups. Each Zr_6 cluster is linked by one bidentate carboxylate from a H_4L_1 ligand to give an 8-connected building unit. For the D_{4h} cluster, an octahedral Zr_6 cluster is capped by eight μ_3 -OH/O atoms, which form an ideal octahedron (Figure S1). Similar D_{2d} and D_{4h} symmetric Zr_6 building units were observed in PCN-225¹⁵ and NU-1000,⁴² respectively. The SPINOL ligand exhibits a tetradentate coordination fashion, binding to four Zr atoms of four Zr_6 cluster via four bidentate carboxylate groups. The bite angle of the SPINOL skeleton in **Spiro-1** is calculated to be 53.4° , which is a little smaller than the angle of 57.3° of the ligand H_4L_1 . As shown in Figure 1b, the framework consists of a large hexagonal bipyramid mesoporous cage with an inner cavity size of $2.3 \times 3.3 \times 3.9$ nm³ (atom-to-atom distance), encapsulated by eight Zr_6 clusters as the vertices and twelve L_1 linkers as the faces that are related by C_3 symmetry. The cage cavities are periodically decorated with the phosphoric acid groups of SPINOL backbones that are accessible to guest molecules. The amphiphilic cage is surrounded by ten adjacent cages with four of them sharing edges and others sharing vertices (Figure S2), thus generating a 3D porous structure with interconnected 1D open channels of 6.1×3.2 Å², 6.1×9.5 Å² and 13.9×13.9 Å² along the a-, b- and c- axis, respectively (Figure 1c).

Spiro-2 crystallizes in the trigonal chiral space group of $P3_221$ with three-second of the formula in the asymmetric unit. It has a similar 3D network to **Spiro-1**, despite their different space group. In contrast to **Spiro-1**, **Spiro-2** contains only one type of 8-connected Zr_6 cluster with D_{2d} symmetry, which may be responsible for the lower symmetry of the whole framework. The framework also possesses a hexagonal bipyramid cage with an inner cavity size of about $2.5 \times 4.1 \times 4.9$ nm³ (atom-to-atom distance) (Figure 1b). When viewed along the a-, b- and c- axis, the porous structure exhibits interconnected 1D open channels of 10.3×6.5 Å², 10.3×14.8 Å² and 18.5×18.5 Å², respectively (Figure S3). To the best of our knowledge, **Spiro-1** and **Spiro-2** are the first two examples of zeolite-like MOFs containing chiral

phosphoric acid functionalities that are beneficial for chiral guest recognition and inclusion.

From the topological viewpoint, the Zr_6 cluster and the SPINOL ligand can be regarded as 8- and 4-connected nodes, respectively. As a result, as shown in Figure 1a, the structures of **Spiro-1** and **Spiro-2** can be simplified as (4,8)-connected net with the point symbol of $\{4^{10}.6^{16}.8^2\}\{4^{12}.6^{14}.8^2\}_2\{4^4.6^2\}_4\{4^5.6\}_2$, herein named **sjt** (Shanghai Jiao Tong University) and now added to the Reticular Chemistry Structure Resource (RCSR) database. By far, a lot of (4,8)-connected MOFs have been reported and most of them exhibit **flu**, **scu**, **sqc** or **csq** topology.^{15,42,44,45} **Spiro-1** and **Spiro-2** represent the first two MOFs with **sjt** net topology. After removing free solvent molecules, the total solvent-accessible volumes of **Spiro-1** and **Spiro-2** are estimated to be 73.2% and 91.7%, respectively, as calculated using the PLATON routine.⁴⁶ To our knowledge, the calculated void space of **Spiro-2** are among the highest values reported for Zr-MOFs and take over the second place in about 70000 reported MOFs (The recorded material is MOF-399⁴⁷ with ca. 94% void space) (Table S12).

Circular dichroism (CD) spectra of **Spiro-1** and **Spiro-2** made from *S* and *R* enantiomers of the corresponding ligand are mirror images of each other, indicative of their enantiomeric nature (Figure S4). The permanent porosity of **Spiro-1** was demonstrated by N_2 adsorption measurements at 77 K. After desolvation of the acetone-exchanged sample by heating at 100 °C under dynamic vacuum overnight, **Spiro-1** remained high crystallinity and exhibit a type I sorption behavior, with a Brunauer–Emmett–Teller (BET) surface area of 2002 m² g⁻¹. In contrast, the evacuated **Spiro-2** almost lost crystallinity (Figure 2c) and exhibited moderate CO_2 adsorption of 140.5 cm³ g⁻¹ (27.8 wt%), but no N_2 adsorption. It is presumably due to the smaller kinetic diameter of CO_2 (3.30 Å) compared to N_2 (3.64 Å), allowing its diffusion in the contracted pore apertures. We also attempted to activate **Spiro-2** through a supercritical CO_2 drying method to avoid capillary forces collapsing the MOF, but still failed to keep its crystallinity. This may be ascribed to the extremely high void space (91.7%) that easily distorts in guest-free state. However, after soaking the activated samples in fresh DMF, the crystallinity of **Spiro-2** can be fully restored (Figure 2c), suggesting that the material went through a structural distortion that is recoverable via re-solvation. This phenomenon is often observed in highly porous MOFs.^{17,47} Dye uptake experiments were then used to certify the structural integrity of the CMOFs in solution. **Spiro-1** and **Spiro-2** can adsorb 4.3 and 5.9 methyl orange (MO, ~ 1.47 nm \times 0.53 nm), and 2.4 and 4.1 rhodamine 6G (~ 1.43 nm \times 1.61 nm) per formula unit in MeOH, respectively (Table S4). In all cases, the inclusion samples gave almost the same PXRD patterns as the pristine sample (Figures 2a,c). The above results implied that the structural integrity and open channels of the two MOFs are maintained in solution.

Chemical Stability. As expected, both **Spiro-1** and **Spiro-2** showed excellent thermal stability. Thermogravimetric analysis (TGA) showed that guest molecules within them could be removed in the temperature ranging from 80 to 140 °C, and the frameworks started to decompose at about 430 °C.

The chemical stability of their frameworks was examined by PXRD and N_2 sorption after treatment in boiling water, 0.01 M NaOH (aq.) and concentrated HCl (aq.) at r.t. for one week, as well as dye uptake measurements. As shown in Figure 2, PXRD patterns of the two CMOFs after these treatments remained intact, suggesting that no phase transition or framework collapse happened. Moreover, in all cases, the **Spiro-2** crystals still displayed strong single-crystal diffractions with almost unchanged unit cell parameter (Figure S7), further confirming the framework stability. Both of the as-treated CMOFs remained permanent porosity, as evidenced by BET measurements (Figures 2b,d). Dye uptake measurements showed the samples of **Spiro-1** and **Spiro-2**

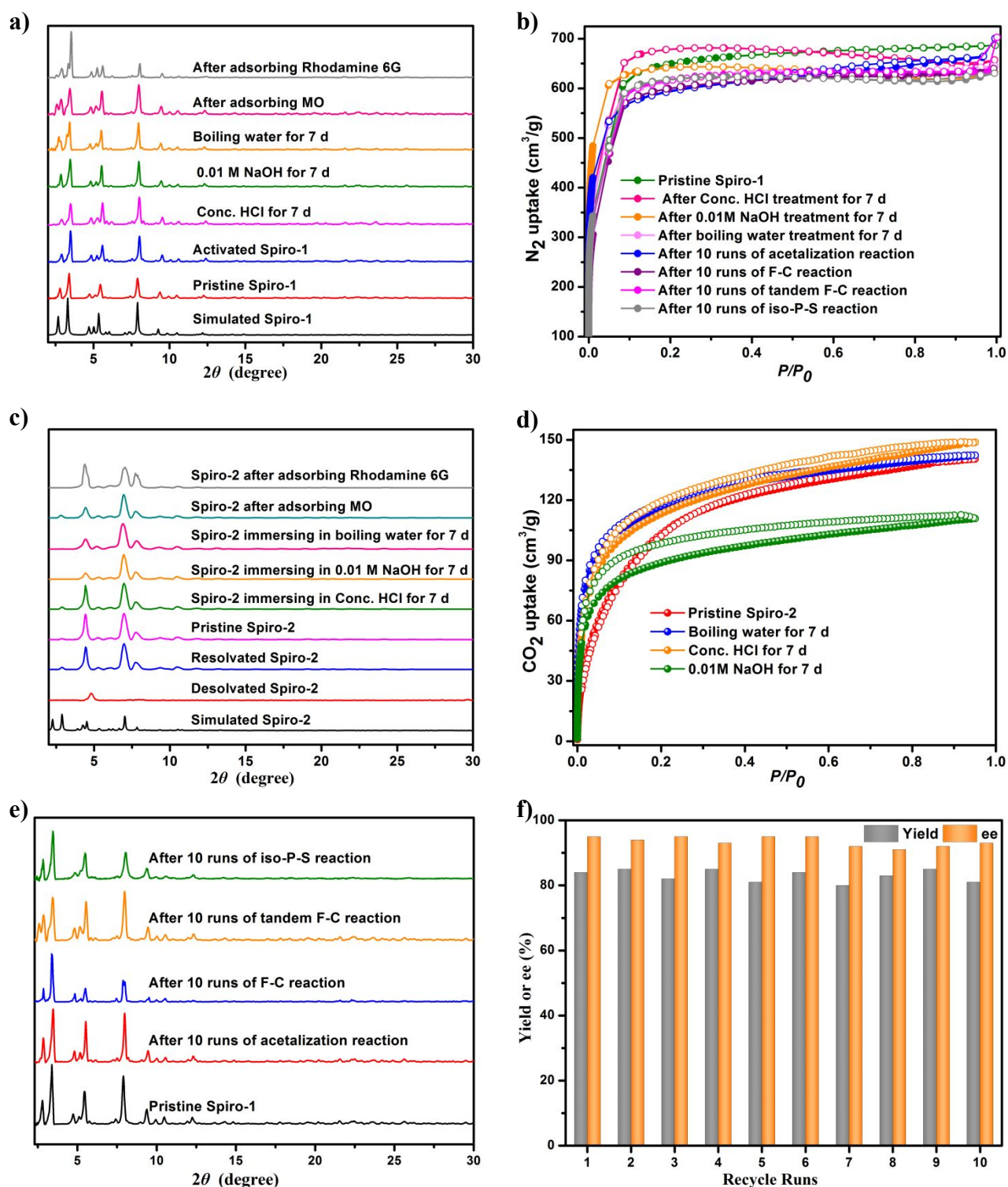


Figure 2. (a) PXRD patterns of **Spiro-1** under different conditions. (b) N_2 adsorption isotherms for **Spiro-1** at 77 K. (c) PXRD patterns of **Spiro-2** under different conditions. (d) CO_2 adsorption isotherms for **Spiro-2** at 273 K, showing the framework stability upon treatment with boiling water, 0.01M NaOH and concentrated HCl. (e) PXRD patterns of **Spiro-1** after 10 recycle runs of catalytic reactions. (f) Recycle results for the **Spiro-1** catalyzed three-component F-C reaction using indole, *p*-bromobenzaldehyde and *p*-toluenesulfonamide as substrates.

after these treatments could adsorb 2.5/2.0/2.2 and 3.4/2.9/3.1 rhodamine 6G per formula unit (Table S4), respectively, comparable to the untreated sample, indicative of the structural integrity. The chemical stability of the present two CMOFs is similar to that reported for similar Zr_6 -based MOFs, which makes

them attractive chiral porous candidates for heterogeneous catalysis and adsorption.

Brønsted acidity. The Brønsted acidity of a solid catalyst is of great importance for catalytic applications. So, we tested the Brønsted acidity of the two Zr -CMOFs as well as the related

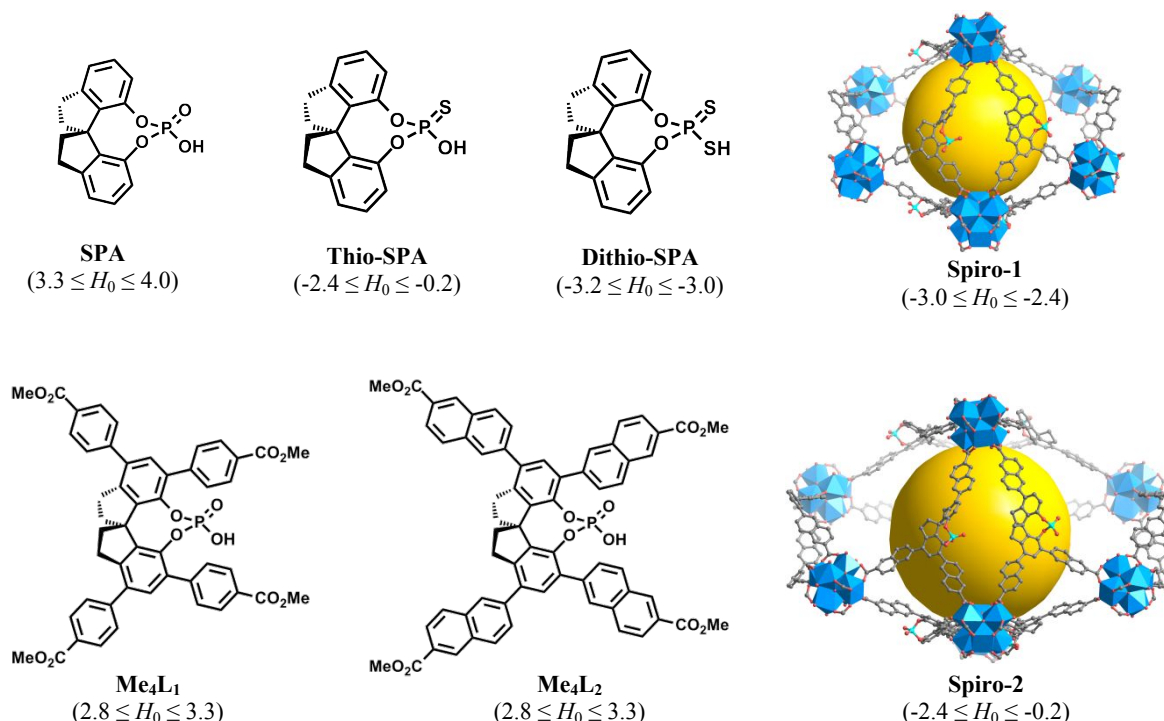


Figure 3. Hammett acidity of some SPINOL-based phosphoric acids, thio- and dithiophosphoric acids and **Spiro-1** and **Spiro-2**.

organic phosphoric acid and their derivatives by the Hammett indicator method.⁴⁸ As shown in Figure 3, the homogeneous catalysts **Me₄L₁** and **Me₄L₂** displayed higher acidity ($2.8 \leq H_0 \leq 3.3$) than the unsubstituted SPINOL phosphoric acid ($3.3 \leq H_0 \leq 4.0$) because of installing electron-withdrawing carboxylate groups on the SPINOL backbone.⁴⁹ After incorporation into MOFs, continue enhancement of the acidity of the SPINOL phosphoric acid was observed ($-3.0 \leq H_0 \leq -2.4$ and $-2.4 \leq H_0 \leq -0.2$ for **Spiro-1** and **Spiro-2**, respectively), which even surpass that of the SPINOL thiophosphoric acid ($-2.4 \leq H_0 \leq -0.2$). Moreover, **Spiro-1** showed a color change even in a benzene solution of 4-nitrodiphenylamine, indicating $H_0 \leq -2.40$ (Table S13), a value approach to the strong SPINOL dithiophosphoric acid ($-3.2 \leq H_0 \leq -3.0$). Besides, the dehydrated **Spiro-1** showed a similar Brønsted acidity ($-3.0 \leq H_0 \leq -2.4$) to the pristine sample, indicating that the water molecules binding to the Zr₆ clusters have no obvious effects on the acidity of the immobilized organocatalysts. The enhanced acidity may be attributed to coordination of carboxylate groups of the linkers to metal ions that withdraws electrons from the SPINOL skeleton, and the isolation of phosphoric acids that prevents the formation of intermolecular hydrogen bonding and promotes proton transfer.⁵⁰ Further study is greatly needed to understand the origin of the Brønsted acidity enhancement of CMOFs.

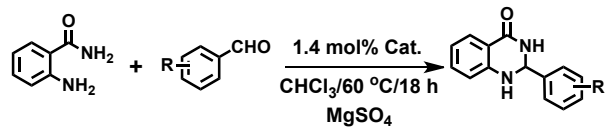
Heterogeneous Catalysis. As mentioned above, chiral phosphoric acids have been found to be excellent asymmetric Brønsted acid catalysts for many meaningful organic transformations.^{32-37,51-54} Meanwhile, the Zr-oxo clusters are shown to be potential catalytically active Lewis acid sites for a number of organic transformations.¹² The large crystalline pore sizes within the two robust CMOFs should provide efficient access to uniformly distributed phosphoric acid sites and Zr₆ cluster and facilitate the transport of reactants and products, which may give rise to high activity and enantioselectivity in different catalytic reactions. This prompted us to evaluate their heterogeneous catalytic behaviors in several different organic transformations.

We first investigated the asymmetric acetalization reaction by the condensation/amine addition cascade sequence, which is one of the most efficient methods for the synthesis of optically active 2,3-dihydroquinazolinones that show extensive important pharmacological activities.⁵⁵ After screening various reaction conditions including catalyst loading, reaction time and temperature (Table S5), we found that, at 1.4 mol% loading, **Spiro-1** could catalyze the condensation/amine addition of 2-aminobenzamide and 4-bromobenzaldehyde to give the product 2,3-dihydroquinazolinone in 99% yield and 96% ee in CHCl₃ at 60 °C after 18 h. Moreover, the electronic nature or positions of the substituent on the aldehyde have limited effects on the catalytic results, and, in all cases, the 2,3-dihydroquinazolinones were obtained in 90-99% yields and 92-99% ee (Table 1, entries 1-8). The chiral nature of the product is dominated by the handedness of the catalyst, as evidenced by that reaction catalyzed by (*R*)-**Spiro-1** gave the *R* enantiomer over the *S* enantiomer (Table 1, entry 2). **Spiro-2** was also effectively in catalyzing the condensation/amine addition of 2-aminobenzamide and aromatic aldehydes, providing almost quantitative yields and 80-90% ee in 10 h. Kinetic study suggested that **Spiro-2** presented higher active than **Spiro-1** (Figure S13). The large pores in **Spiro-2** are thus favorable for substrate and product diffusion, but are unfavorable for high enantiodiscrimination, leading to decreased ee values. Interestingly, in the CMOF catalyst system, we even can detect the imine intermediate during the reaction process, as indicated by ¹H NMR (Figure S14), whereas no imine signal was detected in the homogeneous system. This was probably attributed to the confined cavities in the structure, which may slow down the reaction rate by stabilizing the intermediates via supramolecular interactions.

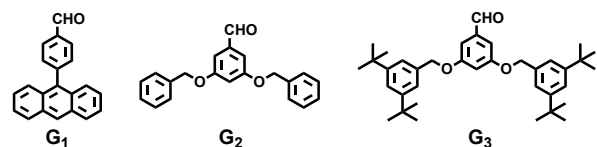
Considering that the coordinated water molecules of Zr₆ clusters can be removed through a thermal activation process, which lead to the exposure of Zr(IV) sites as Lewis acids, we designed a deacetalization/acetalization tandem reaction utilizing both Lewis acid and Brønsted acid sites of the CMOFs. Acetals are highly valuable in organic synthesis because they are capable

of acting as protecting groups for reactive aldehydes, which are one of the most important classes of organic molecules widely used in industry. The open Lewis acidic Zr(IV) and/or phosphoric acid sites in the CMOF promoted the deacetalization of dimethyl or cyclic acetals to aldehydes, which were subsequently converted to optically active 2,3-dihydroquinazolinones catalyzed by chiral phosphoric acids. As shown in Table 2 a broad scope of arylaldehyde dimethyl acetals with different substituents can be

Table 1. Enantioselective Tandem Two-Component Condensation and Cyclization of 2-aminobenzamide with Aldehydes^a



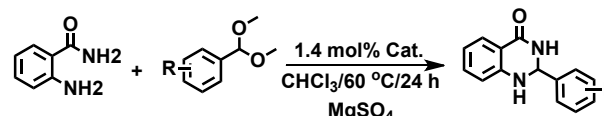
entry	cat.	R	yield (%) ^b	ee (%) ^c
1	(S)-Spiro-1	4-H	96	95
2		4-Br	99 (99) ^d	96 (96) ^d
3		4-Me	94	97
4		4-F	99	95
5		4-NO ₂	99	92
6		3-NO ₂	90	99
7		3-Cl	92	92
8		2-NO ₂	92	98
9		G ₁	73	91
10		G ₂	28	77
11		G ₃	< 8%	n.d.
12	(S)-Me ₄ L ₁ ^e	4-H	99	70
13		4-Br	99	76
14		4-Me	99	71
15		G ₁	99	69
16		G ₂	99	52
17		G ₃	99	n.d.
18	(S)-Spiro-2 ^f	4-H	99	90
19		4-Br	99	87
20		4-Me	99	80
21		4-F	99	85
22		4-NO ₂	99	83
23		3-NO ₂	96	87
24	BINOL-PO ₂ H ^g	4-H	86 (67) ⁱ	86 (26) ⁱ
25	SPINOL-PO ₂ H ^h	4-Br	98	88



^aFor reaction details see experimental section in SI. 1.4 mol% catalyst is the ratio of the MOF formula derived mole amount and the mole amount of 2-aminobenzamide. ^bIsolated yield. ^cDetermined by HPLC. The absolute configurations of the products were assigned as *S* by comparing their HPLC profiles with those reported in literature.⁵⁶ ^dData in brackets are catalyzed by (R)-Spiro-1. ^eCatalyzed by 2.8 mol% (S)-Me₄L₁. ^fReaction time: 10 h. ^gCatalyzed by 10 mol% 3,3'-bis(9-anthracenyl)-BINOL-PO₂H.⁵⁶ ^hCatalyzed by 10 mol% 6,6'-bis(9-anthracenyl)-SPINOL-PO₂H.⁵⁷ ⁱCatalyzed by 10 mol% 3,3'-bis[4-(9-anthracenyl)-2,6-bis(isopropyl)phenyl]-BINOL-PO₂H.⁵⁸ The related catalyst structures and reaction conditions are given in Table S11.

directly converted to 2,3-dihydroquinazolinones in 88-95% yields with 86-97% ee. Besides, cyclic acetals could also undergo the desired transformation to afford the targeted 2,3-dihydroquinazolinones with satisfactory yields (85-96%) and excellent enantioselectivity (83-95%). The yields and ee values compared well with those obtained from the above two-component reaction systems. In addition, under identical conditions, Spiro-2 catalyzed the tandem reactions of dimethyl or cyclic acetals, producing comparable yields (92-98% or 88-96%) but decreased stereoselectivities (77-84% ee or 78-84% ee) in relative to Spiro-1.

Table 2. Enantioselective Tandem Three-Component Deacetalization-Acetalization of 2-aminobenzamide with Arylaldehydes Dimethyl Acetal^a



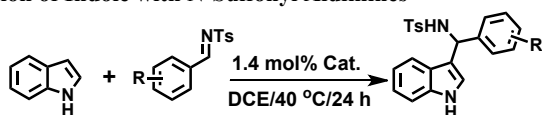
entry	cat.	R	yield (%) ^b	ee (%) ^c
1	(S)-Spiro-1	4-H	95 (79) ^d	92 (90) ^d
2		4-Br	93	94
3		4-Me	90	94
4		4-F	88	91
5		4-NO ₂	89	86
6		3-NO ₂	90	97
7		3-Cl	90	87
8		2-NO ₂	89	93
9		G ₁	70	90
10		G ₂	21	75
11		G ₃	n.r.	n.r.
12	ZrOCl ₂ /(S)-Me ₄ L ₁ ^e	4-H	96	32
13		4-Br	95	32
14		4-Me	94	42
15		G ₁	93	26
16		G ₂	88	24
17		G ₃	85	n.d.
18	(S)-Me ₄ L ₁	4-H	84	75
19		4-Br	83	75
20		4-Me	80	72
21	(S)-Spiro-2 ^f	4-H	98	84
22		4-Br	95	84
23		4-Me	92	77
24	NU-1000 ^g	4-H	n.r.	n.r.

^aFor reaction details see experimental section in SI. The MOF was activated overnight at 220 °C under vacuum to remove coordinated water molecules. 1.4 mol% catalyst is the ratio of the MOF formula derived mole amount and the mole amount of 2-aminobenzamide. ^bDetermined by HPLC. The absolute configurations of the products were assigned as *S* by comparing their HPLC profiles with those reported in literature.⁵⁶ ^cThe data in parentheses are catalyzed by the non-activated Spiro-1. ^dCatalyzed by 2.8 mol% (S)-Me₄L₁ and 8.4 mol% ZrOCl₂. ^eReaction time: 15 h. ^fCatalyzed by 1.4 mol% NU-1000 (activated).

To assess the contribution of the frameworks to the enantioselective catalysis, the activities of related molecular and solid catalysts were examined. When the salt ZrOCl₂ and the activated MOF NU-1000⁴² composing of identical Zr₆ clusters to Spiro-1 was respectively used as catalysts for catalyzing the acetalization and deacetalization-acetalization reactions under identical conditions, no target products were detected by ¹H NMR even after 48 h, suggesting that the Zr₆ clusters in the CMOF were not the active sites for the acetalization transformation. However,

the deacetalization of aldehyde dimethyl acetals and cyclic acetals to aldehydes proceeded smoothly in the presence of ZrOCl_2 or the activated NU-1000, implying that aldehyde formation was catalyzed by the open Lewis acidic Zr(IV) sites in **Spiro-1**. Controlled experiments were also performed for the homogeneous catalyst Me_4L_1 and a mixture of Me_4L_1 and ZrOCl_2 under identical conditions. Both systems were efficient in catalyzing the acetalization and deacetalization-acetalization reactions, but gave the targeted products with much lower enantioselectivities than **Spiro-1** (Table 1, entries 12-14, Table 2, entries 12-14 and 18-20). Additionally, the non-activated **Spiro-1** gave lower yield than the activated sample (79% vs 95%) in catalyzing the deacetalization-acetalization reaction (Table 2, entry 1). Taken together, the above findings indicate that chiral phosphoric acids that together with the Zr_6 clusters and SPINOL rings generate a chiral microenvironment in the MOF, which should be responsible for the observed high catalytic activity and enantioselectivity by concentrating reactants and creating additional steric and electronic effects around the Lewis acid and Brønsted acid sites.

Table 3. Enantioselective Two-Component Friedel-Crafts Reaction of Indole with N-Sulfonyl Aldimines^a



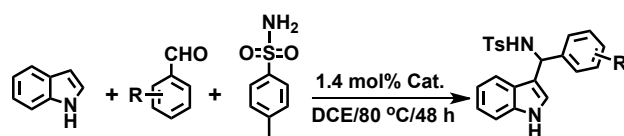
entry	cat.	R	yield (%) ^b	ee (%) ^c
1	(S)-Spiro-1	4-H	98	99
2		4-Br	99	99.9
3		4-Me	92	96
4		4-F	98	99.9
5		4-NO ₂	91	95
6		4-CF ₃	99	99.9
7		2-Cl	94	98
8		1-naphthyl	92	99
9		G ₁	81	99
10		G ₂	26	86
11		G ₃	n.r.	n.r.
12	(S)-Me ₄ L ₁ ^d	4-H	88	96
13		4-Br	91	90
14		4-Me	85	95
15		G ₁	86	98
16		G ₂	67	75
17		G ₃	44	n.d.
18	(S)-Spiro-2 ^e	4-H	97	99
19		4-Br	95	97
20		4-Me	95	93
21	BINOL-PO ₂ H ^f	4-Br	71	82
22	SPINOL-PO ₂ H ^g	4-H	98	98

^aFor reaction details see experimental section in SI. 1.4 mol% catalyst is the ratio of the MOF formula derived mole amount and the mole amount of imine. ^bIsolated yield. ^cDetermined by HPLC. The absolute configurations of the products were assigned as *S* by comparing their HPLC profiles with those reported in literature.³⁵ ^dCatalyzed by 2.8 mol% (S)-Me₄L₁. ^eReaction time: 14 h. ^fCatalyzed by 10 mol% 3,3'-bis(1-naphthyl)-BINOL-PO₂H.³⁵ ^gCatalyzed by 2 mol% of 6,6'-bis(2-naphthyl)-SPINOL-PO₂H.⁵⁹ The related catalyst structures and reaction conditions are given in Table S11.

Several experiments were performed to demonstrate the heterogeneity and recyclability of the MOF catalyst. First, upon completion of the acetalization of 2-aminobenzamide and 4-bromobenzaldehyde, **Spiro-1** could be recovered by simple filtration and reused at least 10 times without any obvious loss of the activity and enantioselectivity (Figure S9). Second, after 10

catalytic cycles, both the PXRD pattern and BET surface area (1849 m² g⁻¹) of **Spiro-1** remained almost the same as those of the pristine sample (Figures 2b and 2e), indicating the robustness of the framework. Third, removal of **Spiro-1** by hot filtration of the reaction mixture after 4 h completely shut down the reaction, suggesting that the supernatant is inactive in promoting the reaction. Inductively coupled plasma mass spectrometric (ICP-MS) analysis of the product solution showed almost no loss of Zr ions (< 0.002%) from the structure per cycle. Final, to probe the role of the pore in catalysis, three sterically demanding substrates were subjected to the acetalization and deacetalization-acetalization reactions. As shown in Tables 1 and 2, the yield gradually decreases when the size of the aldehyde substrate increases. For the largest substrate of 3,5-bis[3,5-di(*tert*-butyl)benzyloxy] benzaldehyde (14 × 21 Å²), only < 8% conversion of the targeted product was detected after 72 h for both of the two reactions,

Table 4. Enantioselective Tandem Three-Component Friedel-Crafts Reaction of Indole with Aldehydes and *p*-Toluenesulfonamide^a



entry	cat.	R	yield (%) ^b	ee (%) ^c
1	(S)-Spiro-1	4-H	87	96
2		4-Br	86	95
3		4-Me	90	96
4		4-F	83	96
5		4-NO ₂	89	95
6		4-CF ₃	87	96
7		2-Cl	92	96
8		1-naphthyl	95	99
9		G ₁	80	98
10		G ₂	20	84
11		G ₃	n.r.	n.r.
12	ZrOCl ₂ /(S)-Me ₄ L ₁ ^d	4-H	19	33
13		4-Br	25	31
14		4-Me	26	25
15		G ₁	29	46
16		G ₂	18	45
17		G ₃	< 5%	n.d.
18	(S)-Spiro-2 ^e	4-H	89	96
19		4-Br	92	93
20		4-Me	92	97
21	NU-1000 ^f	4-H	n.r.	n.r.
22	(S)-Me ₄ L ₁ ^g	4-H	n.r.	n.r.

^aFor reaction details see experimental section in SI. The MOF was activated overnight at 220°C under vacuum to remove coordinated water molecules. 1.4 mol% catalyst is the ratio of the MOF formula derived mole amount and the mole amount of aldehyde. ^bIsolated yield. ^cDetermined by HPLC. The absolute configurations of the products were assigned as *S* by comparing their HPLC profiles with those reported in literature.³⁵ ^dCatalyzed by 2.8 mol% (S)-Me₄L₁ and 8.4 mol% ZrOCl_2 . ^eReaction time: 40 h. ^fCatalyzed by 1.4 mol% NU-1000 (activated). ^gCatalyzed by 2.8 mol% (S)-Me₄L₁.

which was much lower than ~99% yield obtained with Me₄L₁. This extremely low conversion is presumably because the large substrate cannot access the catalytic Brønsted acid sites in the cavity of the MOF through the windows (13.9 × 13.9 Å²) due to its large diameter (14 × 21 Å²), indicating that catalysis occurs mainly at the active sites within the inner pores. Several tests also confirmed that **Spiro-1** was a heterogeneous and recyclable

catalyst in catalyzing two and three-component F-C alkylation and iso-P-S reactions (Figures 2f, S10 and S11).

Spiro-1 was also highly efficient in promoting the asymmetric Friedel-Crafts (F-C) alkylation of indole with N-sulfonyl aryl aldimines, which can provide direct access to enantiopure indole scaffolds that are common structural motifs found in a number of pharmaceuticals and natural products.³⁵ Specially, the reaction of N-sulfonyl aldimine and indole in the presence of 1.4 mol% **Spiro-1** gave the desired product in 98% isolated yield and 99% ee in DCE at 40 °C after 24 h. A range of substituted aryl aldimines were tested under the optimal conditions to expand the reaction scope, and all of them afforded the targeted 3-indolylmethanamine derivatives in 91-99% yields with 95-99.9% ee. Controlled experiments showed that the homogeneous control Me_4L_1 (2.8 mol% loading) gave lower reactivity and enantioselectivity than the solid catalyst, illustrating the superiority of the MOF catalyst. **Spiro-2** catalyzed the F-C reactions in nearly quantitative yields with up to 99% ee, as shown in Table 3 (entries 18-20), indicating pore sizes of the the framework have limited effects on the F-C reactions.

To take advantage of the Lewis acidity of Zr(IV) sites in the CMOF catalyst, we performed the one-pot three-component tandem reaction by using indole, aldehydes and *p*-toluenesulfonamide as the substrates. To our delight, the CMOF could serve as a heterogeneous catalyst for condensation of aromatic aldehydes and *p*-toluenesulfonamide followed by enantioselective F-C alkylation of indole with N-sulfonyl aldimines to afford the targeted 3-indolylmethanamine derivatives (Table 4). The open Zr(IV) sites capable of promoting the condensation of aldehyde and *p*-toluenesulfonamide to N-sulfonyl aldimines was suggested by that both ZrOCl_2 and the activated NU-1000 were active in catalyzing the condensation reaction (~50% conversion). After optimizing the reaction conditions, the one-pot tandem reactions using 1.4 mol% loading of **Spiro-1** as the catalyst was performed in DCE at 80 °C for 48 h. Aromatic aldehydes with both electron-donating and electron-withdrawingsubstituents proceeded smoothly to afford the targeted tandem products in 83-95% yields and 95-99% ee, which are comparable to those obtained from the above non-tandem reactions. It also should be noted that **Spiro-2** promoted the three component tandem reactions to give comparable yields and enantioselectivities to **Spiro-1**, indicating the framework pore sizes have limited confinement effects on the tested F-C reactions.

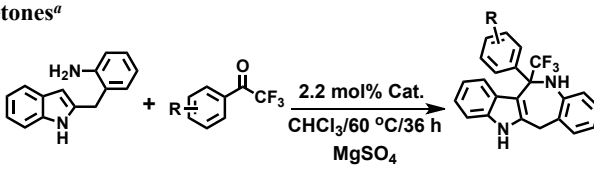
Under otherwise identical conditions, when only Me_4L_1 , ZrOCl_2 or the activated NU-1000 alone was used as a catalyst to catalyze the three-component F-C reaction, no targeted product was observed at all. Moreover, when water was added to the reaction catalyzed by the activated **Spiro-1**, almost no targeted product was detected. When the mixture of Me_4L_1 and ZrOCl_2 was used to catalyze the three-component F-C reactions, in all cases the main products were identified as bis(indolyl)methanes (BIMs) and the F-C products were obtained in 19-26% yields and 25-33% ee (Table 4, entries 12-14), which were much lower than those obtained with **Spiro-1**. This may be ascribed to the coordination of Zr(IV) ions with Me_4L_1 to form metal phosphates, as indicated by ^{31}P NMR spectra (Figure S12), which significantly decreases Lewis acidity of Zr(IV) ions and Brønsted acidity of phosphoric acids and shows a decreased ability to catalyze the asymmetric F-C reactions. Again, these results suggested that the well-defined chiral cavities formed by two different catalytic acid centers in the CMOF to implement the two- and three-component tandem F-C reactions with high efficiency and enantioselectivity.

Several tests also proved the heterogeneous nature of **Spiro-1** in the two- and three-component F-C reactions. The CMOF catalyst can also be readily recycled and reused with negligible loss of

efficiency and enantioselectivity (Figures S10 and 2f), and the recovered catalyst retained crystallinity and remained structurally intact, as revealed by PXRD and BET surface area measurements (Figures 2b and 2e). Moreover, as shown in Tables 3 (entries 9-11) and 4 (entries 9-11), both reactions catalyzed by **Spiro-1** greatly depend on the substrate size: as the size of the aldehyde increases, the yield steadily decreases (80, 20 and 0%). In each case, the yield for the largest aldehyde is much lower than that produced by Me_4L_1 , indicating that the reaction was associated with the substrate being bound in the pore.

We have also demonstrated that the two CMOFs were capable of catalyzing more asymmetric organic transformations. For example, they were effective Brønsted acid catalysts in catalyzing the iso-Pictet-Spengler (P-S) reactions of *o*-aminobenzylindole with various trifluoromethyl ketones, which can give access to biologically important N-containing heterocyclic compounds bearing cyclic quaternary stereocenters with a $-\text{CF}_3$ moiety.⁵⁹ In the presence of 2.2 mol% of **Spiro-1** or **Spiro-2**, the reaction between *o*-aminobenzylindole and phenyl trifluoromethyl ketone proceeded smoothly to give the desired cyclization product in 87-98% isolated yields and 89-96% ee in CHCl_3 at 60 °C after

Table 5. Enantioselective Two-Component iso-Pictet-Spengler Reaction of *o*-amino-benzylindole with Trifluoromethylated Ketones^a



entry	cat.	R	yield (%) ^b	ee (%) ^c
1	(S)-Spiro-1	4-H	94	91
2		4-F	94	90
3		4-Me	87	89
4		4-CF ₃	98	96
5		4-Cl	92	96
6		4-Br	92	96
7		3-F	98	90
8	(S)-Me ₄ L ₁ ^d	4-H	88	90
9		4-F	90	90
10		4-Me	81	82
11	(S)-Spiro-2 ^e	4-H	97	92
12		4-Br	95	95
13		4-Me	90	90
14	SPINOL-PO ₂ H ^f	4-CF ₃	92	93

^aFor reaction details see experimental section in SI. 2.2 mol% catalyst is the ratio of the MOF formula derived mole amount and the mole amount of indole.

^bIsolated yield. ^cDetermined by HPLC. The absolute configurations of the products were assigned as *S* by comparing their HPLC profiles with those reported in literature.⁶⁰ ^dCatalyzed by 4.4 mol% (S)-Me₄L₁. ^eReaction time: 20 h. ^fCatalyzed by 5 mol% 6,6'-bis(3,5-trifluoromethyl)-SPINOL-PO₂H.⁶⁰ The related catalyst structures and reaction conditions are given in Table S11.

36 h. The ee values are comparable to those obtained with the homogeneous counterpart (Table 5, entries 8-10). **Spiro-1** was also proven to be heterogeneous and recyclable catalyst for the iso-P-S reactions (Figure S11 and Figures 2b,e). Besides, the CMOFs can also serve as Brønsted acid catalysts for the catalytic arylation of indole⁶¹ (Table S8) and oxidative dearomatization of naphthol (Table S9).⁶² Further research on using our CMOF catalysts with different acid active centers for related tandem catalysis is in progress.

To allow their recyclable uses, intensive efforts have been focused on immobilizing chiral phosphoric acids on amorphous solid supports such as linear and dendrimer-like polymers and

porous organic polymers, but the reported catalyst systems generally suffer from the disadvantages of low catalyst loading, uneven catalytic sites and typically unsatisfactory enantioselectivity.^{63–66} In particular, a pair of Brønsted acidic MOFs have been constructed from enantiopure BINOL phosphoric acid-derived ligands and Cu₂(carboxylate)₄ building units and used as catalyst to catalyze F-C alkylation of indole with aldimines, but with much lower activity (20–45% yields) and enantioselectivity (6–44% ee) than **Spiro-1**.²⁹ Notably, there are no chiral heterogeneous phosphoric acids catalysts having been reported for enantioselectively catalyzing acetalization and iso-P-S reactions. The 6,6'-bis-9-anthracenyl-spinol phosphoric acid and 6,6'-bis-(3,5-trifluoromethylphenyl)-spinol phosphoric acid were shown to afford the best stereoselectivities for the acetalization reactions of 2-aminobenzamide and aldehydes and iso-P-S reactions of *o*-amino-benzylindole with trifluoromethylated ketones with 80–98% ee and 87–96% ee, respectively, which are comparable to the results of the **Spiro-1** catalyst. So, high enantioselectivities are salient features of our Brønsted acidic CMOF-based protocol, which are among the highest ee values having been reported for homogeneous enantiopure phosphoric acid catalysts.^{35,57,60}

CONCLUSIONS

We have designed a strategy for direct installation of the chiral phosphoric acid sites in Zr(IV)-MOFs by protecting them from coordinating to metal clusters via the incorporation of bulky functional groups at the 6,6'-positions of the enantiopure SPINOL backbone. The CMOFs with the same topological structure displayed excellent chemical stability in acidic, neutral and alkaline aqueous solutions. Incorporation of the chiral phosphoric acid catalysts into porous frameworks led to significant enhancement of their Brønsted acidity. The CMOFs exhibited high reactivity, enantioselectivity and recyclability in heterogeneous Brønsted acid-catalyzed two-component tandem transformations such as acetalization, F-C and iso-P-S reactions and Lewis and Brønsted acid-catalyzed three-component tandem transformations such as deacetalization-acetalization and F-C reactions. This work thus provides a new strategy for preparing heterogeneous Brønsted acid catalysts combining high catalytic reactivity, stereoselectivity and durability and would facilitate the rational design of novel porous multifunctional materials for heterogeneous catalysis, molecular adsorption and separation.

ASSOCIATED CONTENT

Supporting Information.

Experimental procedures and characterization data. This material is available free of charge via the Internet at <http://pubs.acs.org>.

AUTHOR INFORMATION

Corresponding Author

*yongcui@sjtu.edu.cn

*liuy@sjtu.edu.cn

ORCID

Wei Gong: 0000-0002-1458-054X

Yong Cui: 0000-0003-1977-0470

Yan Liu: 0000-0002-7560-519X

Notes

The authors declare no competing financial interest.

ACKNOWLEDGMENTS

We acknowledge many helpful discussions with Professor Qilin Zhou and Jianhua Xie (Nankai University, China). This work was

financially supported by the National Science Foundation of China (Grants 21522104, 21620102001, 21875136, and 91856204), the National Key Basic Research Program of China (2016YFA 0203400), Key Project of Basic Research of Shanghai (17JC1403100 and 18JC1413200) and Shanghai Rising-Star Programe (19QA1404300).

REFERENCES

- (1) Gupta, P.; Paul, S. Solid Acids: Green Alternatives for Acid Catalysis. *Catal. Today* **2014**, *236*, 153–170.
- (2) Davis, M. E. Ordered Porous Materials for Emerging Applications. *Nature* **2002**, *417*, 813–821.
- (3) Jiang, J. C.; Yaghi, O. M. Brønsted Acidity in Metal-Organic Frameworks. *Chem. Rev.* **2015**, *115*, 6966–6997.
- (4) Jiang, J. C.; Gándara, F.; Zhang, Y. B.; Na, K.; Yaghi, O. M. Klemperer, W. G. Superacidity in Sulfated Metal-Organic Framework-808. *J. Am. Chem. Soc.* **2014**, *136*, 12844–12847.
- (5) Li, B. Y.; Leng, K. Y.; Zhang, Y. M.; Dynes, J. J.; Wang, J.; Hu, Y. F.; Ma, D. X.; Shi, Z.; Zhu, L. K.; Zhang, D. L.; Sun, Y. Y.; Chrzanowski, M.; Ma, S. Q. Metal-Organic Framework Based upon the Synergy of a Brønsted Acid Framework and Lewis Acid Centers as a Highly Efficient Heterogeneous Catalyst for Fixed-Bed Reactions. *J. Am. Chem. Soc.* **2015**, *137*, 4243–4248.
- (6) Liang, J.; Liang, Z. B.; Zou, R. Q.; Zhao, Y. L. Heterogeneous Catalysis in Zeolites, Mesoporous Silica, and Metal-Organic Frameworks. *Adv. Mater.* **2017**, *29*, 1701139.
- (7) Su, F.; Guo, Y. H. Advancements in Solid Acid Catalysts for Biodiesel Production. *Green Chem.* **2014**, *16*, 2934–2957.
- (8) Furukawa, H.; Cordova, K. E.; O'Keeffe, M.; Yaghi, O. M. The Chemistry and Applications of Metal-Organic Frameworks. *Science* **2013**, *341*, 974.
- (9) Hendon, C. H.; Rieth, A. J.; Korzyński, M. D.; Dincă, M. Grand Challenges and Future Opportunities for Metal-Organic Frameworks. *ACS Cent. Sci.* **2017**, *3*, 554–563.
- (10) Liu, Y.; Xuan, W.; Cui, Y. Engineering Homochiral Metal-Organic Frameworks for Heterogeneous Asymmetric Catalysis and Enantioselective Separation. *Adv. Mater.* **2010**, *22*, 4112–4135.
- (11) Yuan, S.; Qin, J.; Lollar, C. T.; Zhou, H. C. Stable Metal-Organic Frameworks with Group 4 Metals: Current Status and Trends. *ACS Cent. Sci.* **2018**, *4*, 440–450.
- (12) Rimoldi, M.; Howarth, A. J.; DeStefano, M. R.; Lin, L.; Goswami, S.; Li, P.; Hupp, J. T.; Farha, O. M. Catalytic Zirconium/Hafnium-Based Metal-Organic Frameworks. *ACS Catal.* **2017**, *7*, 997–1014.
- (13) Cavka, J. H.; Jakobsen, S.; Olsbye, U.; Guillou, N.; Lamberti, C.; Bordiga, S.; Lillerud, K. P. A New Zirconium Inorganic Building Brick Forming Metal Organic Frameworks with Exceptional Stability. *J. Am. Chem. Soc.* **2008**, *130*, 13850–13851.
- (14) Férey, G.; Mellot-Draznieks, C.; Serre, C.; Millange, F.; Dutour, J.; Surlé, S.; Margiolaki, I. A Chromium Terephthalate-Based Solid with Unusually Large Pore Volumes and Surface Area. *Science* **2005**, *309*, 2040–2042.
- (15) Jiang, H. L.; Feng, D. W.; Wang, K. C.; Gu, Z. Y.; Wei, Z. W.; Chen, Y. P.; Zhou, H. C. An Exceptionally Stable, Porphyrinic Zr Metal-Organic Framework Exhibiting pH-Dependent Fluorescence. *J. Am. Chem. Soc.* **2013**, *135*, 13934–13938.
- (16) Banerjee, M.; Das, S.; Yoon, M.; Choi, H. J.; Hyun, M. H.; Park, S. M.; Seo, G.; Kim, K. Postsynthetic Modification Switches an Achiral Framework to Catalytically Active Homochiral Metal-Organic Porous Materials. *J. Am. Chem. Soc.* **2009**, *131*, 7524–7525.
- (17) Falkowski, J. M.; Sawano, T.; Zhang, T.; Tsun, G.; Chen, Y.; Lockard, J. V.; Lin, W. B. Privileged Phosphine-Based

- Metal-Organic Frameworks for Broad-Scope Asymmetric Catalysis. *J. Am. Chem. Soc.* **2014**, *136*, 5213–5216.
- (18) Tan, C. X.; Han, X.; Li, Z. J.; Liu, Y.; Cui, Y. Controlled Exchange of Achiral Linkers with Chiral Linkers in Zr-Based UiO-68 Metal-Organic Framework. *J. Am. Chem. Soc.* **2018**, *140*, 16229–16236.
- (19) Xia, Q. C.; Li, Z. J.; Tan, C. X.; Liu, Y.; Gong, W.; Cui, Y. Multivariate Metal-Organic Frameworks as Multifunctional Heterogeneous Asymmetric Catalysts for Sequential Reactions. *J. Am. Chem. Soc.* **2017**, *139*, 8259–8266.
- (20) Wu, C. D.; Hu, A. G.; Zhang, L.; Lin, W. B. A Homochiral Porous Metal-Organic Framework for Highly Enantioselective Heterogeneous Asymmetric Catalysis. *J. Am. Chem. Soc.* **2005**, *127*, 8940–8941.
- (21) Cho, S. H.; Ma, B. Q.; Nguyen, S. T.; Hupp, J. T.; Albrecht-Schmitt, T. E. A Metal-Organic Framework Material that Functions as an Enantioselective Catalyst for Olefin Epoxidation. *Chem. Commun.* **2006**, 2563–2565.
- (22) Dang, D. B.; Wu, P. Y.; He, C.; Xie, Z.; Duan, C. Y. Homochiral Metal-Organic Frameworks for Heterogeneous Asymmetric Catalysis. *J. Am. Chem. Soc.* **2010**, *132*, 14321–14323.
- (23) Gedrich, K.; Heitbaum, M.; Notzon, A.; Senkovska, I.; Fröhlich, R.; Getzschmann, J.; Mueller, U.; Glorius, F.; Kaskel, S. A Family of Chiral Metal-Organic Frameworks. *Chem. Eur. J.* **2011**, *17*, 2099–2106.
- (24) Jeong, K. S.; Go, Y. B.; Shin, S.; Lee, S. M.; Kim, J.; Yaghi, O. M.; Jeong, N. Asymmetric Catalytic Reactions by NbO-Type Chiral Metal-Organic Frameworks. *Chem. Sci.* **2011**, *2*, 877–882.
- (25) Tanaka, K.; Sakuragi, K.; Ozaki, H.; Takada, Y. Highly Enantioselective Friedel-Crafts Alkylation of N,N-dialkylanilines with Trans- β -nitrostyrene Catalyzed by a Homochiral Metal-Organic Framework. *Chem. Commun.* **2018**, *54*, 6328–6331.
- (26) Zhang, Z. X.; Ji, Y. R.; Wojtas, L.; Gao, W. Y.; Ma, S. Q.; Zaworotko, M. J.; Antilla, J. C. Two Homochiral Organocatalytic Metal Organic Materials with Nanoscopic Channels. *Chem. Commun.* **2013**, *49*, 7693–7695.
- (27) Lun, D. J.; Waterhouse, G. I. N.; Telfer, S. G. A General Thermolabile Protecting Group Strategy for Organocatalytic Metal-Organic Frameworks. *J. Am. Chem. Soc.* **2011**, *133*, 5806–5809.
- (28) Ingleson, M. J.; Barrio, J. P.; Bacsá, J.; Dickinson, C.; Park, H.; Rosseinsky, M. J. Generation of a Solid Brønsted Acid Site in a Chiral Framework. *Chem. Commun.* **2008**, 1287–1289.
- (29) Zheng, M.; Liu, Y.; Wang, C.; Liu, S. B.; Lin, W. B. Cavity-Induced Enantioselectivity Reversal in a Chiral Metal-Organic Framework Brønsted Acid Catalyst. *Chem. Sci.* **2012**, *3*, 2623–2627.
- (30) Shimizu, G. K. H.; Vaidhyanathan, R.; Taylor, J. M. Phosphonate and Sulfonate Metal Organic Frameworks. *Chem. Soc. Rev.* **2009**, *38*, 1430–1449.
- (31) Rhaderwick, T.; Zhao, H. S.; Hirschle, P.; Döblinger, M.; Bueken, B.; Reinsch, H.; Vos, D. D.; Wuttke, S.; Kolb, U.; Stock, N. Highly Stable and Porous Porphyrin-Based Zirconium and Hafnium Phosphonates-Electron Crystallography as an Important Tool for Structure Elucidation. *Chem. Sci.* **2018**, *9*, 5467–5478.
- (32) Zamfir, A.; Schenker, S.; Freund, M.; Tsogoeva, S. B.; Chiral BINOL-Derived Phosphoric Acids: Privileged Brønsted Acid Organocatalysts for C-C Bond Formation Reactions. *Org. Biomol. Chem.* **2010**, *8*, 5262–5276.
- (33) Rahman, A.; Lin, X. F. Development and Application of Chiral Spirocyclic Phosphoric Acids in Asymmetric Catalysis. *Org. Biomol. Chem.* **2018**, *16*, 4753–4777.
- (34) Kikuchi, J.; Momiyama, N.; Terada, M. Chiral Phosphoric Acid Catalyzed Diastereo- and Enantioselective Mannich-Type Reaction between Enamides and Thiazolones. *Org. Lett.* **2016**, *18*, 2521–2523.
- (35) Kang, Q.; Zhao, Z. A.; You, S. L. Highly Enantioselective Friedel-Crafts Reaction of Indoles with Imines by a Chiral Phosphoric Acid. *J. Am. Chem. Soc.* **2007**, *129*, 1484–1485.
- (36) He, L.; Laurent, G.; Rétailleau, P.; Folléas, B.; Brayer, J. L.; Masson, G. Highly Enantioselective Aza-Diels-Alder Reaction of 1-Azadienes with Enecarbamates Catalyzed by Chiral Phosphoric Acids. *Angew. Chem. Int. Ed.* **2013**, *52*, 11088–11091.
- (37) Huang, D.; Xu, F. X.; Lin, X. F.; Wang, Y. G. Highly Enantioselective Pictet-Spengler Reaction Catalyzed by SPINOL Phosphoric Acids. *Chem. Eur. J.* **2012**, *18*, 3148–3152.
- (38) Xie, J. H.; Zhou, Q. L. Magical Chiral Spiro Ligands. *Acta Chim. Sinica.* **2014**, *72*, 778–797.
- (39) Huang, Y. B.; Liang, J.; Wang, X. S.; Cao, R. Multifunctional Metal-Organic Framework Catalysts: Synergistic Catalysis and Tandem Reactions. *Chem. Soc. Rev.* **2017**, *46*, 126–157.
- (40) Cao, C. C.; Chen, C. X.; Wei, Z. W.; Qiu, Q. F.; Zhu, N. X.; Xiong, Y. Y.; Jiang, J. J.; Wang, D. W.; Su, C. Y. Catalysis through Dynamic Spacer Installation of Multivariate Functionalities in Metal-Organic Frameworks. *J. Am. Chem. Soc.* **2019**, *141*, 2589–2593.
- (41) Wei, Z. W.; Gu, Z. Y.; Arvapally, R. K.; Chen, Y. P.; Jr. R. N. M.; Lv, J. F.; Yakovenko, A. A.; Feng, D. W.; Omary, M. A.; Zhou, H. C. Rigidifying Fluorescent Linkers by Metal-Organic Framework Formation for Fluorescence Blue Shift and Quantum Yield Enhancement. *J. Am. Chem. Soc.* **2014**, *136*, 8269–8276.
- (42) Mondloch, J. E.; Bury, W.; Fairen-Jimenez, D.; Kwon, S.; DeMarco, E. J.; Weston, M. H.; Sarjeant, A. A.; Nguyen, S. T.; Stair, P. C.; Snurr, R. Q.; Farha, O. M.; Hupp, J. T. Vapor-Phase Metalation by Atomic Layer Deposition in a Metal-Organic Framework. *J. Am. Chem. Soc.* **2013**, *135*, 10294–10297.
- (43) Kalidindi, S. B.; Nayak, S.; Briggs, M. E.; Jansat, S.; Katsoulidis, A. P.; Miller, G. J.; Warren, J. E.; Antypov, D.; Corà, F.; Slater, B.; Prestly, M. R.; Martí-Gastaldo, C.; Rosseinsky, M. J. Chemical and Structural Stability of Zirconium-based Metal-Organic Frameworks with Large Three-Dimensional Pores by Linker Engineering. *Angew. Chem. Int. Ed.* **2015**, *54*, 221–226.
- (44) He, Y. B.; Zhang, Z. J.; Xiang, S. C.; Fronczek, F. R.; Krishna, R.; Chen, B. L. A Microporous Metal-Organic Framework for Highly Selective Separation of Acetylene, Ethylene, and Ethane from Methane at Room Temperature. *Chem. Eur. J.* **2012**, *18*, 613–619.
- (45) Wang, H.; Dong, X. L.; Lin, J. Z.; Teat, S. J.; Jensen, S.; Cure, J.; Alexandrov, E. V.; Xia, Q. B.; Tan, K.; Wang, Q. L.; Olson, D. H.; Proserpio, D. M.; Chabal, Y. J.; Thonhauser, T.; Sun, J. L.; Li, J. Topologically Guided Tuning of Zr-MOF Pore Structures for Highly Selective Separation of C6 Alkane Isomers. *Nat. Commun.* **2018**, *9*, 1745.
- (46) Spek, A. L. Single-Crystal Structure Validation with the Program PLATON. *J. Appl. Crystallogr.* **2003**, *36*, 7.
- (47) Furukawa, H.; Go, Y. B.; Ko, N.; Park, Y. K.; Uribe-Romo, F. J.; Kim, J.; O’Keeffe, M.; Yaghi, O. M. Isoreticular Expansion of Metal-Organic Frameworks with Triangular and Square Building Units and the Lowest Calculated Density for Porous Crystals. *Inorg. Chem.* **2011**, *50*, 9147–9152.
- (48) Walling, C. The Acid Strength of Surfaces. *J. Am. Chem. Soc.* **1950**, *72*, 1164–1168.
- (49) Zhou, F. T.; Yamamoto, H. A Powerful Chiral Phosphoric Acid Catalyst for Enantioselective Mukaiyama-Mannich Reactions. *Angew. Chem. Int. Ed.* **2016**, *55*, 8970–8974.
- (50) Jeong, N. C.; Samanta, B.; Lee, C. Y.; Farha, O. M.; Hupp, J. T. Coordination-Chemistry Control of Proton Conductivity in the Iconic Metal-Organic Framework Material HKUST-1. *J. Am. Chem. Soc.* **2012**, *134*, 51–54.

- (51) Akiyama, T. Stronger Brønsted Acids. *Chem. Rev.* **2007**, *107*, 5744–5758.
- (52) Terada, M. Chiral Phosphoric Acids as Versatile Catalysts for Enantioselective Transformations. *Synthesis* **2010**, 1929–1982.
- (53) Parmar, D.; Sugiono, E.; Raja, S.; Rueping, M. Complete Field Guide to Asymmetric BINOL-Phosphate Derived Brønsted Acid and Metal Catalysis: History and Classification by Mode of Activation; Brønsted Acidity, Hydrogen Bonding, Ion Pairing, and Metal Phosphates. *Chem. Rev.* **2014**, *114*, 9047–9153.
- (54) Parmar, D.; Sugiono, E.; Raja, S.; Rueping, M. Addition and Correction to Complete Field Guide to Asymmetric BINOL-Phosphate Derived Brønsted Acid and Metal Catalysis: History and Classification by Mode of Activation; Brønsted Acidity, Hydrogen Bonding, Ion Pairing, and Metal Phosphates. *Chem. Rev.* **2017**, *117*, 10608–10620.
- (55) Chinigo, G. M.; Paige, M.; Grindrod, S.; Hamel, E.; Dakshanamurthy, S.; Chruszcz, M.; Minor, W.; Brown, M. L. Asymmetric Synthesis of 2,3-Dihydro-2-arylquinazolin-4-ones: Methodology and Application to a Potent Fluorescent Tubulin Inhibitor with Anticancer Activity. *J. Med. Chem.* **2008**, *51*, 620–4631.
- (56) Rueping, M.; Antonchick, A. P.; Sugiono, E.; Grenader, K. Asymmetric Brønsted Acid Catalysis: Catalytic Enantioselective Synthesis of Highly Biologically Active Dihydroquinazolinones. *Angew. Chem. Int. Ed.* **2009**, *48*, 908–910.
- (57) Huang, D.; Li, X. J.; Xu, F. X.; Li, L. H.; Lin, X. F. Highly Enantioselective Synthesis of Dihydroquinazolinones Catalyzed by SPINOL-Phosphoric Acids. *ACS Catal.* **2013**, *3*, 2244–2247.
- (58) Cheng, X.; Vellalath, S.; Goddard, R.; List, B. Direct Catalytic Asymmetric Synthesis of Cyclic Aminals from Aldehydes. *J. Am. Chem. Soc.* **2008**, *130*, 15786–15787.
- (59) Xing, C. H.; Liao, Y. X.; Ng, J.; Hu, Q. S. Optically Active 1,1'-Spirobiindane-7,7'-diol (SPINOL)-Based Phosphoric Acids as Highly Enantioselective Catalysts for Asymmetric Organocatalysis. *J. Org. Chem.* **2011**, *76*, 4125–4131.
- (60) Li, X. J.; Chen, D.; Gu, H. R.; Lin, X. F. Enantioselective Synthesis of Benzazepinoindoles Bearing Trifluoromethylated Quaternary Stereocenters Catalyzed by Chiral Spirocyclic Phosphoric Acids. *Chem. Commun.* **2014**, *50*, 7538–7541.
- (61) Qi, L. W.; Mao, J. H.; Zhang, J.; Tan, B. Organocatalytic Asymmetric Arylation of Indoles Enabled by Azo Groups. *Nat. Chem.* **2018**, *10*, 58–64.
- (62) Zhu, G. M.; Bao, G. J.; Li, Y. P.; Yang, J. X.; Sun, W. S.; Li, J.; Hong, L.; Wang, R. Chiral Phosphoric Acid Catalyzed Asymmetric Oxidative Dearomatization of Naphthols with Quinones. *Org. Lett.* **2016**, *18*, 5288–5291.
- (63) Kundu, D. S.; Schmidt, J.; Bleschke, C.; Thomas, A.; Blechert, S. A Microporous Binol-Derived Phosphoric Acid. *Angew. Chem., Int. Ed.* **2012**, *51*, 5456–5459.
- (64) Rueping, M.; Sugiono, E.; Steck, A.; Theissmann, T. Synthesis and Application of Polymer-Supported Chiral Brønsted Acid Organocatalysts. *Adv. Synth. Catal.* **2010**, *352*, 281–287.
- (65) Almenara, L. C.; Etsch, C. R.; Planes, L. O.; Pericàs, M. A. Polystyrene-Supported TRIP: A Highly Recyclable Catalyst for Batch and Flow Enantioselective Allylation of Aldehydes. *ACS Catal.* **2016**, *6*, 7647–7651.
- (66) Zhang, X.; Kormos, A.; Zhang, J. Self-Supported BINOL-Derived Phosphoric Acid Based on a Chiral Carbazolic Porous Framework. *Org. Lett.* **2017**, *19*, 6072–6075.

Graphic Content

